Variational Monte Carlo analysis of the Hubbard model with a confining potential: one-dimensional fermionic optical lattice systems

Yusuke FUJIHARA,[1] Akihisa KOGA[1] and Norio KAWAKAMI[1,2]

[1]*Department of Applied Physics, Osaka University, Suita, Osaka 565-0871, Japan*
[2]*Department of Physics, Kyoto University, Kyoto 606-8502, Japan*

We investigate the one-dimensional Hubbard model with a confining potential, which may describe cold fermionic atoms trapped in an optical lattice. Combining the variational Monte Carlo simulations with the new stochastic reconfiguration scheme proposed by Sorella, we present an efficient method to systematically treat the ground state properties of the confined system with a site-dependent potential. By taking into account intersite correlations as well as site-dependent on-site correlations, we are able to describe the coexistence of the metallic and Mott insulating regions, which is consistent with other numerical results. Several possible improvements of the trial states are also addressed.

KEYWORDS: variational Monte Carlo, fermionic Hubbard model, optical lattice, ultracold atoms

1. Introduction

Strongly correlated particle systems have attracted much interest. Among them, recent advances in laser cooling techniques make it possible to confine cold atoms in an artificial lattice, the so-called optical lattice.[1,2] By tuning the amplitude and the direction of the laser, the hopping integral between sites and the strength of the confining potential can be controlled. Furthermore, by means of the Feshbach resonance,[3] the interaction between particles is also controlled, which thereby stimulates intensive experimental investigations on the effect of particle correlations in the optical lattice.

Bosonic systems have been discussed intensively[4–8] since the discovery of the superfluid-Mott insulator transition in the confined system with rubidium ions.[1] The ground state properties of the system have theoretically been studied in detail.[9–16] Recently a degenerate Fermi gas with potassium ions (also lithium) is also realized,[17–24] which stimulates further investigations on strongly correlated fermionic systems in the optical lattice.[25–27]

Theoretical analyses of the fermionic systems have been done by means of the numerical techniques such as the quantum Monte Carlo (QMC) method[28–30] and the density matrix renormalization group (DMRG).[31,32] It has been elucidated that the metallic regions coexist with the Mott insulating regions in the one-dimensional (1D) confined system with large interactions.[28,29,31] However, these numerical methods face serious problems when they are applied to the 2D and 3D systems. The DMRG method enables us to obtain the precise results only for the 1D systems, and the QMC method usually suffers from the minus sign problems for a large-cluster system. Therefore, it is highly desirable to find a powerful method to investigate the fermionic confined systems systematically.

One of the potential methods suitable for this purpose may be the variational Monte Carlo (VMC) calculation,[33–36] which allows us to study not only 1D but also 2D and 3D systems in the same framework. However, we again encounter some problems when the VMC method is extended to the confined systems with a site-dependent potential. One of the most serious problems is that a large number of variational parameters should be treated in order to correctly describe the ground state properties. Therefore, it is necessary to introduce sophisticated techniques beyond the standard ones used so far in variational theory.

In this paper, we present an efficient method based on the VMC simulations that is tractable and applicable to the optical lattice systems. To overcome the above-mentioned difficulty inherent in the confined systems, we make use of a stochastic reconfiguration with Hessian acceleration (SRH) scheme to minimize the ground state energy in a given parameter space. This method was recently proposed by Sorella[37] to discuss long-range electron correlations in the periodic Hubbard system. By taking the 1D Hubbard model with harmonic confinement as a typical example, we will demonstrate that the new stochastic VMC simulations work quite well for the optical lattice system with a confining potential.

This paper is organized as follows. In §2, we introduce the model Hamiltonian and briefly summarize the VMC method with the stochastic reconfiguration scheme. In §3, we apply the VMC simulations to discuss the effect of the particle correlations in the confined system, by using several distinct trial states. A summary and discussions are given in the final section.

2. Model and Method

We consider a strongly correlated fermionic system in the optical lattice. Here, we treat fermionic particles with $s = 1/2$ spin, for simplicity, although a potassium atom ^{40}K, for example, has an $s = 9/2$ spin.[26] In this paper, we restrict our discussions to the 1D model in order to clearly demonstrate the potentiality of our numerical method applicable to the confined systems with a site-dependent potential. The simplified model Hamiltonian

we consider here reads[28,29]

$$\mathcal{H} = -t \sum_{<i,j>\sigma} c^{\dagger}_{i\sigma} c_{j\sigma} + \sum_{i\sigma} V_i n_{i\sigma} + U \sum_i n_{i\uparrow} n_{i\downarrow}, \quad (1)$$

where $c^{\dagger}_{i\sigma}$ ($c_{i\sigma}$) is a creation (annihilation) operator at the ith site with spin $\sigma(=\uparrow,\downarrow)$, and $n_{i\sigma} = c^{\dagger}_{i\sigma} c_{i\sigma}$. t is the nearest neighbor hopping matrix, and $U(>0)$ the on-site repulsive interaction. Interacting fermions are assumed to be trapped by the harmonic potential V_i, where $V_{L/2-1} = V_{L/2} = 0$ at two sites around the center, $V_0 = V_{L-1} = V$ at the edges (L is the length of the system). In the following, we fix $t = 1$ as an energy unit.

In the confined system, the local particle count depends on the site because the confining potential V_i is site-dependent. Namely, the particle density around the center is larger than that around the edge. This suggests that the introduction of the repulsive interaction changes the distribution of various local quantities such as the particle density and the double occupancy. Therefore, the careful treatment of the particle correlations is desirable to clarify the ground state properties.

To this end, we make use of the VMC method.[33–36] In comparison with other numerical methods, it has an advantage in extending the calculation to the 2D and 3D fermionic systems, as mentioned above. This method has successfully been applied to various correlated electron systems with periodic potentials.[38–48]

We introduce here a trial state with Jastrow-type projection operators as[49]

$$|\Psi\rangle = \mathcal{J}|\Phi\rangle, \quad (2)$$

where $|\Phi\rangle$ is the Slater determinant for the noninteracting state and the Jastrow operator $\mathcal{J}$ incorporates two-particle correlations, whose explicit form will be given in the next section. In order to include the effects of the inhomogeneous potential, we should deal with a large number of site-dependent variational parameters. This is contrasted to the standard problems in condensed matter physics,[33–48] where only one or two parameters are sufficient to describe the ground state properties. Although those parameters are invaluable to obtain a more accurate solution in the confined systems, it becomes much more difficult to determine their optimized values.

For optimizing the parameters, there exist some iterative methods. In ordinary iterative methods, the set of parameters $\mathbf{x}$ can be iteratively changed by $\mathbf{x} \to \mathbf{x} + \boldsymbol{\gamma}$. Here $\boldsymbol{\gamma}$ is determined by minimizing the energy

$$\begin{aligned} \Delta E &= E(\mathbf{x}+\boldsymbol{\gamma}) - E(\mathbf{x}) \\ &= \frac{1}{2}\boldsymbol{\gamma}^T B \boldsymbol{\gamma} - \mathbf{f}^T \boldsymbol{\gamma}, \end{aligned} \quad (3)$$

where $\mathbf{f}$ and B denote the first energy derivative and the Hessian matrix. As a result, $\boldsymbol{\gamma}$ is denoted as

$$\boldsymbol{\gamma} = B^{-1}\mathbf{f}. \quad (4)$$

In order to optimize the parameters efficiently, it is important to evaluate $\mathbf{f}$ and B. The SRH scheme, which is based on the iterative methods, allows us to optimize enormous parameters even more efficiently.[37] In comparison with other iterative techniques such as the Powell's method and the quasi-Newton method, it has an advantage in reaching the ground state in a few iterations. The important idea in this scheme is that $\mathbf{f}$ and B are evaluated by using the statistical fluctuations of each projection operator, and in the framework of VMC, the efficient and rapid convergence is achieved. Furthermore, we can introduce an additional free parameter β in the matrix B, which can accelerate the convergence. This parameter originates from the expansion coefficient of the trial wave function, and contributes to the efficiency and the accuracy of the calculation. This scheme was originally introduced to analyze a trial wave function with longer-range density-density or spin-spin correlations in the periodic systems.[37]

In this paper, we extend the SRH scheme so as to treat multivariable trial wave functions including the effects of the inhomogeneous potential. When the site-dependent parameters are introduced, the Hessian matrix B should become positive semidefinite with some zero eigenvalues. This reflects the fact that no particle exists around edges in the confining potential. In this case, some parameters do not contribute to the energy and thus cannot be determined straightforwardly. Therefore, it may be difficult to obtain B^{-1} in eq. (4). To overcome this difficulty, we propose to make use of

$$\boldsymbol{\gamma} = B^{+}\mathbf{f} \quad (5)$$

instead of eq. (4). Here B^{+} is the Moore-Penrose pseudoinverse matrix of B. This matrix is always defined and has similar properties to the inverse matrix. We will demonstrate below that this new stochastic scheme works well and thereby enables us to discuss how particle correlations affect the ground state properties in the confined system.

3. Results

In this section, we perform the VMC simulations with several trial states to clarify the role of the on-site and intersite particle correlations, by which we confirm the potentiality of our method. Here, we deal with the system ($L = 100$) with $N_\uparrow = N_\downarrow = 30$ and $V = 10$, where N_σ is the number of particles with spin σ.

3.1 Gutzwiller paramagnetic state

First, we consider the Gutzwiller paramagnetic trial state, which incorporates the on-site particle correlations. The Gutzwiller trial state[50–52] is explicitly given as

$$|\Psi_G\rangle = \mathcal{P}_G|\Phi_0\rangle, \quad (6)$$

$$\mathcal{P}_G = \exp\left[\sum_i \alpha_i n_{i\uparrow} n_{i\downarrow}\right], \quad (7)$$

where $|\Phi_0\rangle$ is the Slater determinant for the noninteracting paramagnetic ground state. Note that $\alpha_i (i = 0,\ldots,L-1)$ is a site-dependent variational parameter with $\alpha_i = \alpha_{L-i-1}$, which may describe the effect of local correlations in our inhomogeneous system.

By optimizing $L/2(=50)$ variational parameters $\{\alpha_i\}$ by means of the SRH scheme, we calculate local quantities for the confined system. Let us first look at how ef-

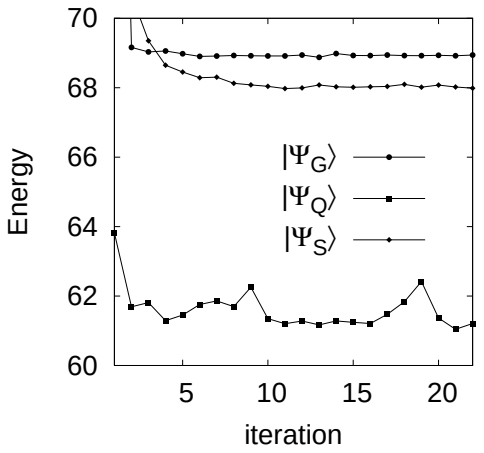

Fig. 1. Calculated energies in each iteration. Filled circles, squares and diamonds are the results obtained from three distinct trial states (see text) when $U = 6$ and $V = 10$.

ficiently our scheme works for optimizing the variational parameters. In Fig. 1, we show the calculated energy as a function of the iteration when it starts from a certain initial state ($|\Psi_Q\rangle$ and $|\Psi_S\rangle$ are defined in the following subsections). For each iteration, we perform the VMC calculation with large samplings ($\sim 500,000$). An important point is that the ground state almost converges in a few iterations, although the energy for each trial state slightly oscillates even after sufficient iterations. We find that this does not depend on the number of the Monte Carlo samplings for each iteration, which implies that statistical errors in our calculations mainly come from this oscillation. Anyway, we find that the stochastic VMC scheme with eq. (5) works quite well for our confined system.

Several physical quantities thus calculated are summarized in Fig. 2. It is found that the introduction of the interaction slightly changes the local particle density $\langle n_i \rangle$, and decreases the local double occupation $\langle n_{i\uparrow} n_{i\downarrow} \rangle$. At the same time, spin fluctuations $\langle (S_i^z - \langle S_i^z \rangle)^2 \rangle$ are enhanced and density fluctuations $\langle (n_i - \langle n_i \rangle)^2 \rangle$ are suppressed. This implies that the repulsive interaction U excludes doubly occupied states at each lattice site. It should be noticed that nearest-neighbor spin correlations $\langle (S_i^z S_{i-1}^z + S_i^z S_{i-1}^z)/2 \rangle$ are strongly enhanced in the two regions around the 30th and 70th sites. In those regions, the average of the particle density is almost unity and density (spin) fluctuations are suppressed (enhanced) strongly. Namely, the repulsive interaction U has a tendency to localize particles and enhance local spin fluctuations, as should be expected.

In this way, the trial state with site-dependent Gutzwiller factors can take into account the local particle correlations to some extent. In fact, the ground state energy obtained from the Gutzwiller trial state eq. (6) is lower than that obtained by the ordinary Hartree-Fock approximation, as shown in Fig. 3. However, we could not reproduce the Mott insulating region that should be spatially extended in a *finite* region, as suggested by other groups.[28,29,31]

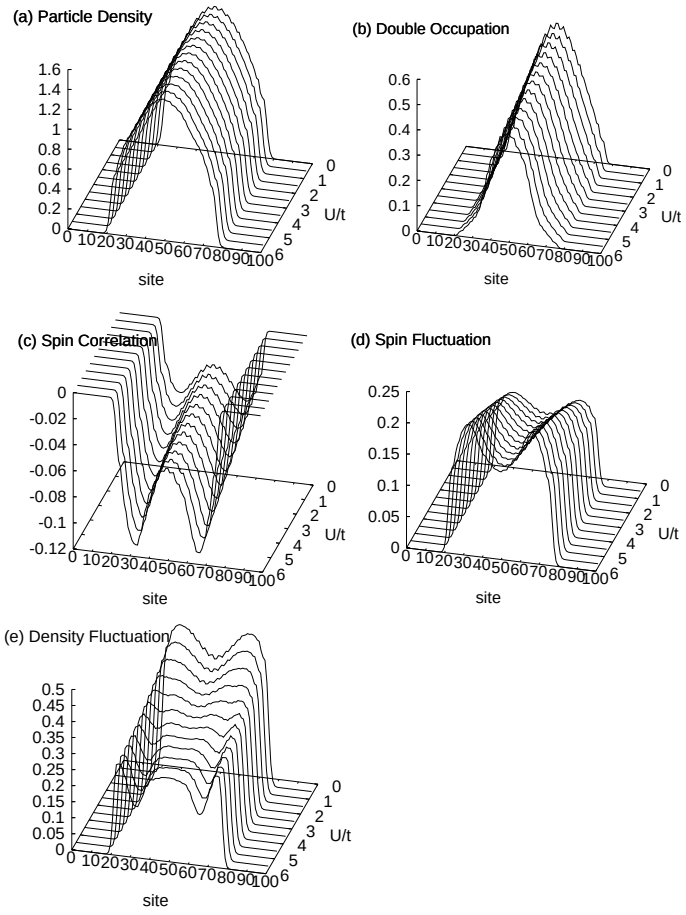

Fig. 2. (a) particle density, (b) double occupation, (c) short-range spin correlation, (d) spin fluctuations, and (e) density fluctuations, which are obtained by the Gutzwiller wave function $|\Psi_G\rangle$.

3.2 Intersite doublon-holon correlations

To take into account the particle correlations more precisely, we introduce the intersite doublon-holon (DH) correlations.[35,36] The corresponding trial state is given as,

$$|\Psi_Q\rangle = \mathcal{P}_Q \mathcal{P}_G |\Phi_0\rangle, \tag{8}$$

$$\mathcal{P}_Q = \exp\left[\alpha' \sum_i \widehat{Q}_i\right], \tag{9}$$

where

$$\widehat{Q}_i = \widehat{D}_i \prod_\tau (1 - \widehat{H}_{i+\tau}) + \widehat{H}_i \prod_\tau (1 - \widehat{D}_{i+\tau}) \tag{10}$$

with $\widehat{D}_i = n_{i\uparrow} n_{i\downarrow}$, $\widehat{H}_i = (1 - n_{i\uparrow})(1 - n_{i\downarrow})$ and τ runs over all the nearest neighbors. The variational parameter α' is assumed to be independent on the sites, for simplicity (see the discussion in 3.3). Note that the doublon-holon projection operator $\mathcal{P}_Q$ takes into account the nearest-neighbor correlations between a doubly occupied site and an empty site, which may be important to stabilize the Mott insulating state.

The ground state energy thus computed is shown in Fig. 3. It is found that the energies obtained from the trial states eqs. (6) and (8) are almost the same in the weak coupling region. On the other hand, in the strong

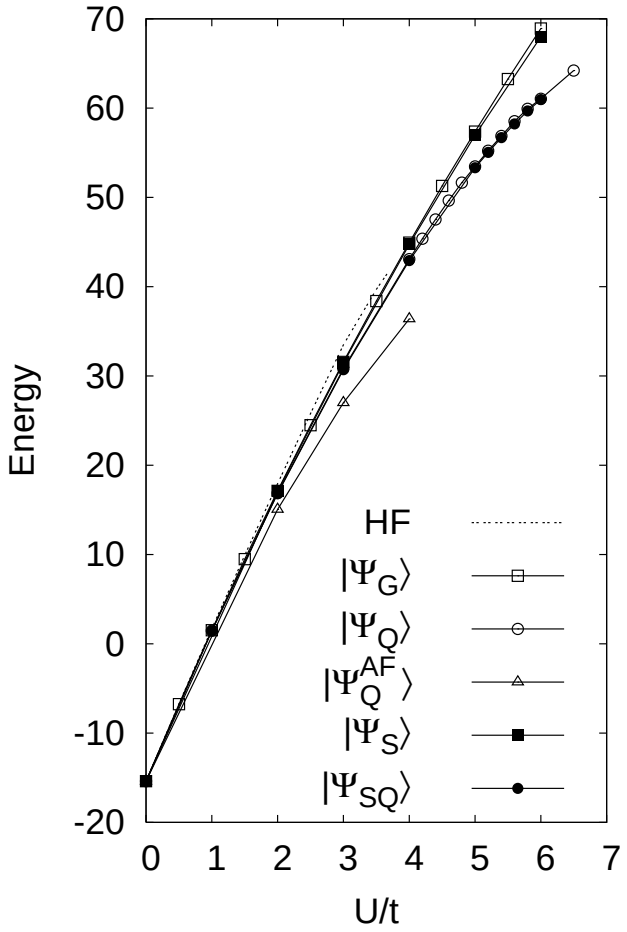

Fig. 3. The ground state energy as a function of the repulsive interaction U. Open squares, open circles, open triangles, filled squares, and filled circles are the results obtained from the Gutzwiller(GW), paramagnetic DH+GW, magnetically ordered DH+GW, SC+GW and SC+DH+GW trial state (see text for each notation). The energy obtained by the Hartree-Fock (HF) approximation is shown by the dotted line, for comparison. Statistical errors originating from stochastic oscillations are less than the size of symbol for each point.

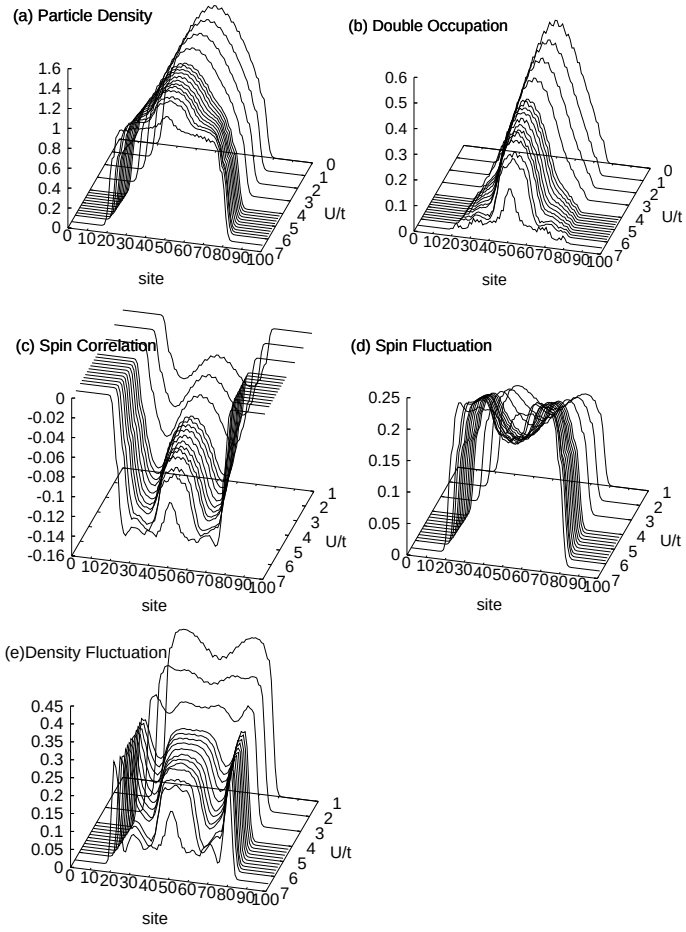

Fig. 4. (a) particle density, (b) double occupation, (c) short range spin correlation, (d) spin fluctuations, and (e) density fluctuations, which are obtained from the DH+GW trial state, $|\Psi_Q\rangle$.

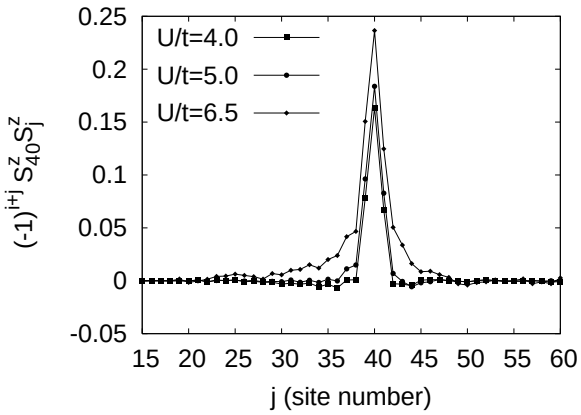

Fig. 5. Staggered long-range spin correlations $(-1)^{i+j} S_i^z S_j^z$ between the 40th site and the jth site. Squares, circles and diamonds are the results for the system with $U = 4.0, 5.0$ and 6.5.

coupling region $U > 4$, we find that the ground state energy for the trial state (8) is lower than the other, implying that the DH correlations play an important role in the region. In fact, characteristic behavior appears in various physical quantities beyond $U = 4$, as shown in Fig. 4. It is seen that when the interaction is increased, the plateau regions appear in the curve of the particle density at $\langle n_i \rangle = 1$, where the double occupancy is suppressed strongly. Furthermore, we find that spin (density) fluctuations are considerably enhanced (suppressed). This implies that the commensurability (half-filling condition) is induced self-consistently due to particle correlations and thus the Mott insulating states are stabilized in *finite* regions in contrast to the results of the Gutzwiller trial state (see Fig. 2).

The emergence of the Mott insulating state is also seen clearly in the two-point spin correlation $(-1)^{i+j}\langle S_i^z S_j^z \rangle$ ($i = 40$ fixed) shown in Fig. 5. At $U = 4$, the local particle density, $\langle n_i \rangle \sim 1.2$, at the 40th site is larger than half filling, which means that the metallic state is realized around there, and therefore the spin correlations are extended up to a few neighbor sites. On the other hand, in the large U case, we find that the spin correlation length becomes much longer, signaling the formation of the Mott insulating state when $U > 6$.

Summarizing, by including on-site and intersite parti-

cle correlations, our variational theory properly reproduces the coexistence phase, which is consistent with those of QMC and DMRG simulations.[28,29,31] Furthermore, by comparing the results obtained from the two trial states eqs. (6) and (8), we can say that intersite DH correlations are essential to describe the coexistence of metallic and Mott insulating states in the confined system.

3.3 Further improvements of the paramagnetic state

Here, we wish to briefly comment on further possible improvements of the trial wave function for the paramagnetic state. We examine a trial state which incorporates the effect of intersite spin correlations. The corresponding trial state we consider is

$$|\Psi_S\rangle = \mathcal{P}_S|\Psi_G\rangle, \tag{11}$$

$$|\Psi_{SQ}\rangle = \mathcal{P}_S|\Psi_Q\rangle. \tag{12}$$

$$\mathcal{P}_S = \exp\left[\sum_i v_i \widehat{\mathcal{S}}_i\right] \tag{13}$$

where the spin correlation operator $\widehat{\mathcal{S}}_i$ is defined as,

$$\widehat{\mathcal{S}}_i = \frac{1}{2}\left(S_i^z S_{i-1}^z + S_i^z S_{i+1}^z\right). \tag{14}$$

The ground state energy calculated for each state is shown in Fig. 3. As seen in the figure, we cannot find a drastic change in the energy (as well as the physical quantities) although a lot of variational parameters for spin correlations are introduced. The results indicate that the nearest-neighbor S^z-S^z spin correlations are not so important in comparison with the DH correlations. We think that $\mathbf{S}_i \cdot \mathbf{S}_{i+1}$ spin correlations or longer-range spin correlations are necessary to improve the trial state.

One may also take into account *site-dependent* DH correlations to improve the trial state as,

$$|\Psi_{Q'}\rangle = \exp\left[\sum_j \alpha_i' \widehat{Q}_i\right]|\Psi_G\rangle. \tag{15}$$

In general, it is difficult to find the ground-state parameters for this wave function in the strong coupling regime even by means of the SRH scheme. Nevertheless, by employing smaller lattice systems, we have checked that the site-dependent DH correlations give similar results to that of the *uniform* DH correlations. Further improvements of the iterative technique should allow us to discuss the effects of the site-dependent DH correlations more precisely, which is now under consideration.

3.4 Examination of the magnetically ordered state

We discuss here the ground state properties by exploiting a trial state including the magnetic order. It is known that the Hubbard model in the periodic lattice without confining potentials has a tendency to stabilize the long-range magnetic order when the particle density satisfies the commensurability, *i.e.* the condition of half filling. In the 1D Hubbard model, however, the real long-range order is not realized[53–56] due to large quantum fluctuations, in contrast to the 2D square-lattice system where the magnetic order is stabilized.[57] Nevertheless, it is expected that the effect of enhanced spin correlations can be incorporated to some extent even in terms of a Hartree-Fock type approximation.

In our inhomogeneous system, the spatially-modulated magnetic properties may show up. Therefore, to examine a trial state with magnetic order, we start with the unrestricted Hartree-Fock (UHF) state, where we determine the spatially modulated particle density and magnetization at each site self-consistently.[58]

The trial state for VMC simulations is then written as

$$|\Psi_Q^{AF}\rangle = \mathcal{P}_Q\mathcal{P}_G|\Phi_{AF}(M)\rangle, \tag{16}$$

where $|\Phi_{AF}(M)\rangle$ is the non-interacting state obtained by the UHF approximation with an additional variational parameter M, which corresponds to the total magnetization. Note that the SRH algorithm can be applied only to the Jastrow-type variational parameters. Therefore, by performing the SRH scheme with a fixed M, we optimize the variational parameters $(\{\alpha_i\}, \alpha')$. We show the particle density $\langle n_i\rangle$ and the average of the staggered magnetization μ in Figs. 6 and 7. The latter quantity is defined as,

$$\mu = \frac{1}{L}\sum_i |\langle n_{i\uparrow}\rangle - \langle n_{i\uparrow}\rangle|. \tag{17}$$

We find that the magnetization is almost zero and little

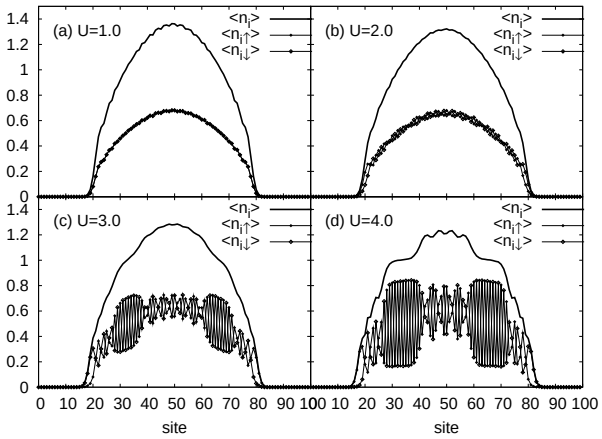

Fig. 6. Filled (open) circles represent the density distributions of particles with ↑ (↓) spin and a solid line the local particle density, when (a) $U = 1.0$, (b) $U = 2.0$, (c) $U = 3.0$, and (d) $U = 4.0$.

difference appears in the spin-dependent density distributions when $U < 2$. This suggests that the paramagnetic ground state is realized in the case. On the other hand, the increase of the interaction yields the spatially-modulated magnetization, as shown in Fig. 6. An important point is that the large staggered magnetization is induced in the vicinity of the $i = 30$th and $i = 70$th sites, where the plateau appears in the curve of the particle density, as shown in Fig. 6. This implies that magnetic correlations are strongly enhanced in the *finite* insulating region, which is consistent with those discussed in the previous subsection.

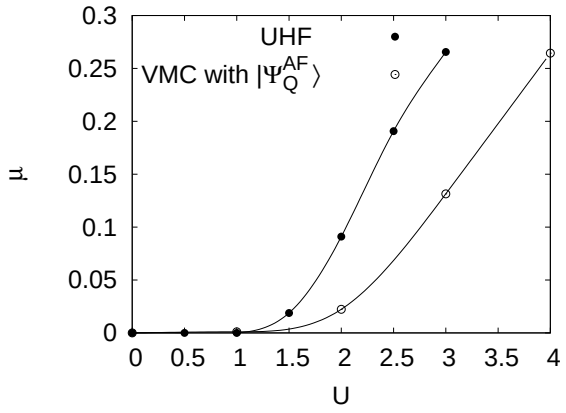

Fig. 7. The average of the staggered magnetization μ as a function of U. Filled and open circles represent the magnetization obtained by the UHF approximation and the VMC method with the trial state $|\Psi_Q^{AF}\rangle$.

Note that the VMC simulations with the HF approximation cannot describe a paramagnetic quantum liquid state correctly in 1D. Nevertheless, we can see that the magnetically ordered state is more stable than the paramagnetic state in the large U region within our VMC analysis (see also Fig. 3). Therefore, if we can properly incorporate quantum fluctuations that suppress the magnetic order in the Hartree-Fock state, we end up with an excellent trial state. Alternatively, starting from the paramagnetic state, we should incorporate spatially extended spin correlations more precisely. These problems are now under consideration.

4. Summary and Discussions

We have investigated correlation effects in the 1D Hubbard model with harmonic confinement, which may be relevant to correlated fermionic systems trapped in the optical lattices. We have aimed at developing an efficient method based on the VMC simulations that is tractable and applicable to the optical lattice systems. One of the central problems to be resolved is how to treat a large number of site-dependent variational parameters.

As a first step to incorporate the effect of particle correlations in such inhomogeneous systems, we have examined a trial state with site-dependent Gutzwiller factors (on-site correlations). By exploiting the stochastic reconfiguration with Hessian acceleration scheme, we were able to treat more than 50 Gutzwiller variational parameters, whereas the standard Gutzwiller approach deals with only one or two parameters. We have thus clarified how the introduction of the repulsive interaction changes the distribution of local quantities. It turns out that although site-dependent correlations are taken into account, the Mott insulating region cannot be properly described only in terms of the on-site Gutzwiller factors.

We have thus improved the trial state by taking into account the intersite DH correlations. It has been elucidated that the coexistence state with metallic and Mott insulating regions emerges for large U in this case, which is consistent with those obtained by other numerical studies. This suggests that the intersite DH correlations are essential to describe the metal-insulator coexistence phase. We have further examined how the intersite spin correlations modify the results, and have found that as far as Ising-type spin correlations are concerned, the results are little changed. Nevertheless, there still remains a possibility to improve the results by incorporating the Heisenberg-type isotropic spin correlations. It has been also shown that the variational treatment starting from the mean-field antiferromagnetic state reasonably reproduces the coexistence of metallic and insulating regions, although the real long-range order should be prohibited due to large quantum fluctuations inherent in 1D systems. In this way, the present scheme is quite flexible, thereby providing us with various ways to improve our variational treatment of the Hubbard model with a site-dependent potential.

In conclusion, we have confirmed that the VMC simulations with numbers of site-dependent parameters can be efficiently performed with the aid of the stochastic acceleration scheme. This demonstrates that the stochastic VMC method provides a powerful tool to treat the correlation effects in optical lattice systems with a site-dependent potential, which have not been easily tractable by conventional optimization procedures. This naturally motivates us to extend our discussions to the 2D and 3D optical lattice systems, which is now under consideration.

Acknowledgment

The numerical computations were carried out at the Supercomputer Center, the Institute for Solid State Physics, University of Tokyo. We would like to thank M. Yamashita for valuable discussion. This work was supported by Grant-in-Aids for Scientific Research [Grant No. 17740226 (AK) and Grant No. 18043017 (NK)] from The Ministry of Education, Culture, Sports, Science and Technology of Japan.

1) M. Greiner, O. Mandel, T. Esslinger, T. W. Hänsch and I. Bloch: Nature (London) **415** (2002) 39.
2) For a review, see Nature (London) **416** (2002) 205-246.
3) S. Inouye, M. R. Andrews, J. Stenger, H. -J. Miesner, D. M. Stamper-Kurn and W. Ketterle: Nature (London) **392** (1998) 151.
4) O. Mandel, M. Greiner, A. Widera, T. Rom, T.W. Hänsch and I, Bloch: Nature (London) **425** (2003) 937.
5) T. Stöferle, H. Moritz, C. Schori, M. Köhl and T. Esslinger: Phys. Rev. Lett. **92** (2004) 130403.
6) B. Paredes, A. Widera, V. Murg, O. Mandel, S. Fölling, I. Cirac, G. V. Shlyapnikov, T.W. Hänsch and I. Bloch: Nature (London) **429** (2004) 277.
7) F. Gerbier, A. Widera, S. Fölling, O. Mandel, T. Gericke and I. Bloch: Phys. Rev. Lett. **95** (2005) 050404.
8) F. Gerbier, S. Fölling, A. Widera, O. Mandel, T. Gericke and I. Bloch: Phys. Rev. Lett. **96** (2006) 090401.
9) D. Jaksch, C. Bruder, J. I. Cirac, C. W. Gardiner and P. Zoller: Phys. Rev. Lett. **81** (1998) 3108.
10) M. W. Jack and M. Yamashita: Phys. Rev. A **67** (2003) 033605.
11) L. Pollet, S. Rombouts, K. Heyde and J. Dukelsky: Phys. Rev. A **69** (2004) 043601.
12) S. Bergkvist, P. Henelius, and A. Rosengren: Phys. Rev. A **70** (2004) 053601.
13) D. L. Kovrizhin, G. Venketeswara, and S. Sinha: Europhys. Lett. **72** (2005) 162.

14) V. W. Scarola and S. D. Sarma: Phys. Rev. Lett. **95** (2005) 033003.
15) S. Wessel, F. Alet, S. Trebst, D. Leumann, M. Troyer and G. G. Batrouni: J. Phys. Soc. Jpn **74** (2005) 10.
16) C. Kollath, U. Schollwöck, J. V. Delft and W. Zwerger: Phys. Rev. A **71** (2005) 053606.
17) B. DeMarco and D. S. Jin: Science **285** (1999) 1703.
18) A. G. Truscott, K. E. Strecker, W. I. McAlexander, G. B. Partridge and R. G. Hulet: Science **291** (2001) 2570.
19) F. Schreck, L. Khaykovich, K. L. Corwin, G. Ferrari, T. Bourdel, J. Cubizolles and C. Salomon: Phys. Rev. Lett. **87** (2001) 080403.
20) S. R. Granade, M. Gehm, K. M. O'Hara and J. E. Thomas: Phys. Rev. Lett. **88** (2002) 120405.
21) Z. Hadzibabic, C. A. Stan, K. Dieckmann, S. Gupta, M. W. Zwierlein, A. Görlits and W. Ketterle: Phys. Rev. Lett. **88** (2002) 160401.
22) M. Greiner, C. A. Regal, and D. S. Jin: Nature (London) **429** (2004) 277.
23) M. Bartenstein, A. Altmeyer, S. Riedl, S. Jochim, C. Chin, J. H. Denschlag and R. Grinmm: Phys. Rev. Lett. **92** (2004) 120401.
24) M. W. Zwierlein, C. A. Stan, C. H. Schunck, S. M. F. Raupach, A. J. Kerman and W. Ketterle: Phys. Rev. Lett. **92** (2004) 120403.
25) G. Roati, E. de Mirandes, F. Ferlaino, H. Ott, G. Modugno and M. Inguscio: Phys. Rev. Lett. **92** (2004) 230402.
26) M. Köhl, H. Moritz, T. Stöferle, K. Günter and T. Esslinger: Phys. Rev. Lett. **94** (2005) 080403.
27) T. Stöferle, H. Moritz, K. Günter, M. Köhl and T. Esslinger: Phys. Rev. Lett. **96** (2006) 030401.
28) M. Rigol, A. Muramatsu, G. G. Batrouni and R. T. Scalettar: Phys. Rev. Lett. **91** (2003) 130403.
29) M. Rigol and A. Muramatsu: Phys. Rev. A **69** (2004) 053612.
30) F. K. Pour, M. Rigol, S. Wessel and A. Muramatsu: cond-mat/0608491.
31) T. Yamashita, N. Kawakami and M. Yamashita: unpublished.
32) T. Yamashita, N. Kawakami and M. Yamashita: Phys. Rev. A *in press*.
33) W. L. McMillan: Phys. Rev. **138** (1965) A442 .
34) D. Ceperley, G. V. Chester and K. H. Kalos: Phys. Rev. B **16** (1977) 3081.
35) H. Yokoyama and H. Shiba: J. Phys. Soc. Jpn. **56** (1987) 1490; J. Phys. Soc. Jpn **56** (1987) 3582; J. Phys. Soc. Jpn. **59** (1990) 3669.
36) H. Yokoyama: Prog. Theor. Phys. **108** (2002) 59.
37) S. Sorella: Phys. Rev. B **71** (2005) 241103.
38) T. Giamarchi and C. Thuillier: Phys. Rev. B **42** (1990) 10641; **43** (1991) 12943.
39) A. Oguri and T. Asahata: Phys. Rev. B **46** (1992) 14073.
40) H. Otsuka: J. Phys. Soc. Jpn. **61** (1992) 1645.
41) Y. Liu, J. Dong, C. Gong, and T. Chen: Phys. Rev. B **48** (1993) 1306.
42) T. Watanabe, H. Yokoyama, Y. Tanaka and J. Inoue: J. Phys. Soc. Jpn. **75** (2006) 074707.
43) S. Kuratani, A. Koga, and N. Kawakami: unpublished.
44) K. Kobayashi and H. Yokoyama: J. Phys. Chem. Solid **66** (2005) 1384.
45) A. Koga, N. Kawakami, H. Yokoyama, and K. Kobayashi: AIP Conf. Proc. **850** (2006) 1458.
46) T. Watanabe, H. Yokoyama, Y. Tanaka, J. Inoue, and M. Ogata: J. Phys. Soc. Jpn. **73** (2004) 3404.
47) P. G. McQueen and C. S. Wang: Phys. Rev. B **44** (1991) 10021.
48) H. N. Kono and Y. Kuramoto: J. Phys. Soc. Jpn. **75** (2006) 084706.
49) R. Jastrow: Phys. Rev. **98** (1955) 1479.
50) M. C. Gutzwiller: Phys. Rev. Lett. **10** (1963) 159; Phys. Rev. **134** (1964) A923.
51) T. A. Kaplan, P. Horsch and P. Flude: Phys. Rev. Lett. **49** (1982) 889.
52) P. Fazekas and K. Penc: Int. J. Mod. Phys. B **2** (1988) 485.
53) E. H. Lieb and F. Y. Wu: Phys. Rev. Lett. **20** (1968) 1445.
54) M. Takahashi: Prog. Theor. Phys. **42** (1969) 1098; **45** (1971) 756.
55) H. Shiba: Phys. Rev. B **6** (1972) 930.
56) T. Usuki, N. Kawakami and A. Okiji: Phys. Lett. **135A** (1989) 476.
57) J. E. Hirsch: Phys. Rev. Lett. **51** (1983) 1900; Phys. Rev. B **31** (1985) 4403.
58) N. Furukawa and M. Imada: J. Phys. Soc. Jpn. **60** (1991) 3669.